Letter

Study of light scalar mesons through $D_s^+ \to \pi^0\pi^0 e^+\nu_e$ and $K_S^0 K_S^0 e^+\nu_e$ decays

M. Ablikim,[1] M. N. Achasov,[10,b] P. Adlarson,[68] S. Ahmed,[14] M. Albrecht,[4] R. Aliberti,[28] A. Amoroso,[67a,67c] M. R. An,[32] Q. An,[64,50] X. H. Bai,[58] Y. Bai,[49] O. Bakina,[29] R. Baldini Ferroli,[23a] I. Balossino,[24a] Y. Ban,[39,h] K. Begzsuren,[26] N. Berger,[28] M. Bertani,[23a] D. Bettoni,[24a] F. Bianchi,[67a,67c] J. Bloms,[61] A. Bortone,[67a,67c] I. Boyko,[29] R. A. Briere,[5] H. Cai,[69] X. Cai,[1,50] A. Calcaterra,[23a] G. F. Cao,[1,55] N. Cao,[1,55] S. A. Cetin,[54a] J. F. Chang,[1,50] W. L. Chang,[1,55] G. Chelkov,[29,a] D. Y. Chen,[6] G. Chen,[1] H. S. Chen,[1,55] M. L. Chen,[1,50] S. J. Chen,[35] X. R. Chen,[25] Y. B. Chen,[1,50] Z. J. Chen,[20,i] W. S. Cheng,[67c] G. Cibinetto,[24a] F. Cossio,[67c] X. F. Cui,[36] H. L. Dai,[1,50] X. C. Dai,[1,55] A. Dbeyssi,[14] R. E. de Boer,[4] D. Dedovich,[29] Z. Y. Deng,[1] A. Denig,[28] I. Denysenko,[29] M. Destefanis,[67a,67c] F. De Mori,[67a,67c] Y. Ding,[33] C. Dong,[36] J. Dong,[1,50] L. Y. Dong,[1,55] M. Y. Dong,[1,50,55] X. Dong,[69] S. X. Du,[72] Y. L. Fan,[69] J. Fang,[1,50] S. S. Fang,[1,55] Y. Fang,[1] R. Farinelli,[24a] L. Fava,[67b,67c] F. Feldbauer,[4] G. Felici,[23a] C. Q. Feng,[64,50] J. H. Feng,[51] M. Fritsch,[4] C. D. Fu,[1] Y. Gao,[64,50] Y. Gao,[39,h] Y. G. Gao,[6] I. Garzia,[24a,24b] P. T. Ge,[69] C. Geng,[51] E. M. Gersabeck,[59] A. Gilman,[62] K. Goetzen,[11] L. Gong,[33] W. X. Gong,[1,50] W. Gradl,[28] M. Greco,[67a,67c] L. M. Gu,[35] M. H. Gu,[1,50] C. Y. Guan,[1,55] A. Q. Guo,[25] A. Q. Guo,[22] L. B. Guo,[34] R. P. Guo,[41] Y. P. Guo,[9,f] A. Guskov,[29,a] T. T. Han,[42] W. Y. Han,[32] X. Q. Hao,[15] F. A. Harris,[57] K. L. He,[1,55] F. H. Heinsius,[4] C. H. Heinz,[28] Y. K. Heng,[1,50,55] C. Herold,[52] M. Himmelreich,[11,d] T. Holtmann,[4] G. Y. Hou,[1,55] Y. R. Hou,[55] Z. L. Hou,[1] H. M. Hu,[1,55] J. F. Hu,[48,j] T. Hu,[1,50,55] Y. Hu,[1] G. S. Huang,[64,50] L. Q. Huang,[65] X. T. Huang,[42] Y. P. Huang,[1] Z. Huang,[39,h] T. Hussain,[66] N. Hüsken,[22,28] W. Ikegami Andersson,[68] W. Imoehl,[22] M. Irshad,[64,50] S. Jaeger,[4] S. Janchiv,[26] Q. Ji,[1] Q. P. Ji,[15] X. B. Ji,[1,55] X. L. Ji,[1,50] Y. Y. Ji,[42] H. B. Jiang,[42] X. S. Jiang,[1,50,55] J. B. Jiao,[42] Z. Jiao,[18] S. Jin,[35] Y. Jin,[58] M. Q. Jing,[1,55] T. Johansson,[68] N. Kalantar-Nayestanaki,[56] X. S. Kang,[33] R. Kappert,[56] M. Kavatsyuk,[56] B. C. Ke,[72] I. K. Keshk,[4] A. Khoukaz,[61] P. Kiese,[28] R. Kiuchi,[1] R. Kliemt,[11] L. Koch,[30] O. B. Kolcu,[54a,m] B. Kopf,[4] M. Kuemmel,[4] M. Kuessner,[4] A. Kupsc,[37,68] M. G. Kurth,[1,55] W. Kühn,[30] J. J. Lane,[59] J. S. Lange,[30] P. Larin,[14] A. Lavania,[21] L. Lavezzi,[67a,67c] Z. H. Lei,[64,50] H. Leithoff,[28] M. Lellmann,[28] T. Lenz,[28] C. Li,[40] C. H. Li,[32] Cheng Li,[64,50] D. M. Li,[72] F. Li,[1,50] G. Li,[1] H. Li,[64,50] H. Li,[44] H. B. Li,[1,55] H. J. Li,[15] H. N. Li,[48,j] J. L. Li,[42] J. Q. Li,[4] J. S. Li,[51] Ke Li,[1] L. K. Li,[1] Lei Li,[3] P. R. Li,[31,k,l] S. Y. Li,[53] W. D. Li,[1,55] W. G. Li,[1] X. H. Li,[64,50] X. L. Li,[42] Xiaoyu Li,[1,55] Z. Y. Li,[51] H. Liang,[64,50] H. Liang,[1,55] H. Liang,[27] Y. F. Liang,[46] Y. T. Liang,[25] G. R. Liao,[12] L. Z. Liao,[1,55] J. Libby,[21] C. X. Lin,[51] D. X. Lin,[25] T. Lin,[1] B. J. Liu,[1] C. X. Liu,[1] D. Liu,[14,64] F. H. Liu,[45] Fang Liu,[1] Feng Liu,[6] G. M. Liu,[48,j] H. M. Liu,[1,55] Huanhuan Liu,[1] Huihui Liu,[16] J. B. Liu,[64,50] J. L. Liu,[65] J. Y. Liu,[1,55] K. Liu,[1] K. Y. Liu,[33] Ke Liu,[17] L. Liu,[64,50] M. H. Liu,[9,f] P. L. Liu,[1] Q. Liu,[55] Q. Liu,[69] S. B. Liu,[64,50] T. Liu,[1,55] W. M. Liu,[64,50] X. Liu,[31,k,l] Y. Liu,[31,k,l] Y. B. Liu,[36] Z. A. Liu,[1,50,55] Z. Q. Liu,[42] X. C. Lou,[1,50,55] F. X. Lu,[51] H. J. Lu,[18] J. D. Lu,[1,55] J. G. Lu,[1,50] X. L. Lu,[1] Y. Lu,[1] Y. P. Lu,[1,50] C. L. Luo,[34] M. X. Luo,[71] P. W. Luo,[51] T. Luo,[9,f] X. L. Luo,[1,50] X. R. Lyu,[55] F. C. Ma,[33] H. L. Ma,[1] L. L. Ma,[42] M. M. Ma,[1,55] Q. M. Ma,[1] R. Q. Ma,[1,55] R. T. Ma,[55] X. X. Ma,[1,55] X. Y. Ma,[1,50] F. E. Maas,[14] M. Maggiora,[67a,67c] S. Maldaner,[4] S. Malde,[62] Q. A. Malik,[66] A. Mangoni,[23b] Y. J. Mao,[39,h] Z. P. Mao,[1] S. Marcello,[67a,67c] Z. X. Meng,[58] J. G. Messchendorp,[56] G. Mezzadri,[24a] T. J. Min,[35] R. E. Mitchell,[22] X. H. Mo,[1,50,55] N. Yu. Muchnoi,[10,b] H. Muramatsu,[60] S. Nakhoul,[11,d] Y. Nefedov,[29] F. Nerling,[11,d] I. B. Nikolaev,[10,b] Z. Ning,[1,50] S. Nisar,[8,g] Q. Ouyang,[1,50,55] S. Pacetti,[23b,23c] X. Pan,[9,f] Y. Pan,[59] A. Pathak,[1] A. Pathak,[27] P. Patteri,[23a] M. Pelizaeus,[4] H. P. Peng,[64,50] K. Peters,[11,d] J. Pettersson,[68] J. L. Ping,[34] R. G. Ping,[1,55] S. Pogodin,[29] R. Poling,[60] V. Prasad,[64,50] H. Qi,[64,50] H. R. Qi,[53] M. Qi,[35] T. Y. Qi,[9] S. Qian,[1,50] W. B. Qian,[55] Z. Qian,[51] C. F. Qiao,[55] J. J. Qin,[65] L. Q. Qin,[12] X. P. Qin,[9] X. S. Qin,[42] Z. H. Qin,[1,50] J. F. Qiu,[1] S. Q. Qu,[36] K. H. Rashid,[66] K. Ravindran,[21] C. F. Redmer,[28] A. Rivetti,[67c] V. Rodin,[56] M. Rolo,[67c] G. Rong,[1,55] Ch. Rosner,[14] M. Rump,[61] H. S. Sang,[64] A. Sarantsev,[29,c] Y. Schelhaas,[28] C. Schnier,[4] K. Schoenning,[68] M. Scodeggio,[24a,24b] W. Shan,[19] X. Y. Shan,[64,50] J. F. Shangguan,[47] M. Shao,[64,50] C. P. Shen,[9] H. F. Shen,[1,55] X. Y. Shen,[1,55] H. C. Shi,[64,50] R. S. Shi,[1,55] X. Shi,[1,50] X. D. Shi,[64,50] J. J. Song,[15] J. J. Song,[42] W. M. Song,[27,1] Y. X. Song,[39,h] S. Sosio,[67a,67c] S. Spataro,[67a,67c] K. X. Su,[69] P. P. Su,[47] F. F. Sui,[42] G. X. Sun,[1] H. K. Sun,[1] J. F. Sun,[15] L. Sun,[69] S. S. Sun,[1,55] T. Sun,[1,55] W. Y. Sun,[27] X. Sun,[20,i] Y. J. Sun,[64,50] Y. Z. Sun,[1] Z. T. Sun,[1] Y. H. Tan,[69] Y. X. Tan,[64,50] C. J. Tang,[46] G. Y. Tang,[1] J. Tang,[51] J. X. Teng,[64,50] V. Thoren,[68] W. H. Tian,[44] Y. T. Tian,[25] I. Uman,[54b] B. Wang,[1] C. W. Wang,[35] D. Y. Wang,[39,h] H. J. Wang,[31,k,l] H. P. Wang,[1,55] K. Wang,[1,50] L. L. Wang,[1] M. Wang,[42] M. Z. Wang,[39,h] Meng Wang,[1,55] S. Wang,[9,f] W. Wang,[51] W. H. Wang,[69] W. P. Wang,[64,50] X. Wang,[39,h] X. F. Wang,[31,k,l] X. L. Wang,[9,f] Y. Wang,[51] Y. D. Wang,[38] Y. F. Wang,[1,50,55] Y. Q. Wang,[1] Y. Y. Wang,[31,k,l] Z. Wang,[1,50] Z. Y. Wang,[1] Ziyi Wang,[55] Zongyuan Wang,[1,55] D. H. Wei,[12] F. Weidner,[61] S. P. Wen,[1] D. J. White,[59] U. Wiedner,[4] G. Wilkinson,[62] M. Wolke,[68] L. Wollenberg,[4] J. F. Wu,[1,55] L. H. Wu,[1] L. J. Wu,[1,55] X. Wu,[9,f] X. H. Wu,[27] Z. Wu,[1,50] L. Xia,[64,50] H. Xiao,[9,f] S. Y. Xiao,[1] Z. J. Xiao,[34] X. H. Xie,[39,h] Y. G. Xie,[1,50] Y. H. Xie,[6] T. Y. Xing,[1,55] C. J. Xu,[51] G. F. Xu,[1] Q. J. Xu,[13] W. Xu,[1,55] X. P. Xu,[47] Y. C. Xu,[55] F. Yan,[9,f] L. Yan,[9,f] W. B. Yan,[64,50] W. C. Yan,[72] H. J. Yang,[43,e] H. X. Yang,[1] L. Yang,[44] S. L. Yang,[55] Y. X. Yang,[12] Yifan Yang,[1,55] Zhi Yang,[25] M. Ye,[1,50] M. H. Ye,[7] J. H. Yin,[1] Z. Y. You,[51] B. X. Yu,[1,50,55] C. X. Yu,[36] G. Yu,[1,55] J. S. Yu,[20,i] T. Yu,[65] C. Z. Yuan,[1,55] L. Yuan,[2] X. Q. Yuan,[39,h] Y. Yuan,[1] Z. Y. Yuan,[51] C. X. Yue,[32] A. A. Zafar,[66]

X. Zeng Zeng,[6] Y. Zeng,[20,i] A. Q. Zhang,[1] B. X. Zhang,[1] Guangyi Zhang,[15] H. Zhang,[64] H. H. Zhang,[51] H. H. Zhang,[27] H. Y. Zhang,[1,50] J. J. Zhang,[44] J. L. Zhang,[70] J. Q. Zhang,[34] J. W. Zhang,[1,50,55] J. Y. Zhang,[1] J. Z. Zhang,[1,55] Jianyu Zhang,[1,55] Jiawei Zhang,[1,55] L. M. Zhang,[53] L. Q. Zhang,[51] Lei Zhang,[35] S. Zhang,[51] S. F. Zhang,[35] Shulei Zhang,[20,i] X. D. Zhang,[38] X. Y. Zhang,[42] Y. Zhang,[62] Y. T. Zhang,[72] Y. H. Zhang,[1,50] Yan Zhang,[64,50] Yao Zhang,[1] Z. Y. Zhang,[69] G. Zhao,[1] J. Zhao,[32] J. Y. Zhao,[1,55] J. Z. Zhao,[1,50] Lei Zhao,[64,50] Ling Zhao,[1] M. G. Zhao,[36] Q. Zhao,[1] S. J. Zhao,[72] Y. B. Zhao,[1,50] Y. X. Zhao,[25] Z. G. Zhao,[64,50] A. Zhemchugov,[29,a] B. Zheng,[65] J. P. Zheng,[1,50] Y. H. Zheng,[55] B. Zhong,[34] C. Zhong,[65] L. P. Zhou,[1,55] Q. Zhou,[1,55] X. Zhou,[69] X. K. Zhou,[55] X. R. Zhou,[64,50] X. Y. Zhou,[32] A. N. Zhu,[1,55] J. Zhu,[36] K. Zhu,[1] K. J. Zhu,[1,50,55] S. H. Zhu,[63] T. J. Zhu,[70] W. J. Zhu,[36] W. J. Zhu,[9,f] Y. C. Zhu,[64,50] Z. A. Zhu,[1,55] B. S. Zou,[1] and J. H. Zou[1]

(BESIII Collaboration)

[1]*Institute of High Energy Physics, Beijing 100049, People's Republic of China*
[2]*Beihang University, Beijing 100191, People's Republic of China*
[3]*Beijing Institute of Petrochemical Technology, Beijing 102617, People's Republic of China*
[4]*Bochum Ruhr-University, D-44780 Bochum, Germany*
[5]*Carnegie Mellon University, Pittsburgh, Pennsylvania 15213, USA*
[6]*Central China Normal University, Wuhan 430079, People's Republic of China*
[7]*China Center of Advanced Science and Technology, Beijing 100190, People's Republic of China*
[8]*COMSATS University Islamabad, Lahore Campus, Defence Road, Off Raiwind Road, 54000 Lahore, Pakistan*
[9]*Fudan University, Shanghai 200443, People's Republic of China*
[10]*G.I. Budker Institute of Nuclear Physics SB RAS (BINP), Novosibirsk 630090, Russia*
[11]*GSI Helmholtzcentre for Heavy Ion Research GmbH, D-64291 Darmstadt, Germany*
[12]*Guangxi Normal University, Guilin 541004, People's Republic of China*
[13]*Hangzhou Normal University, Hangzhou 310036, People's Republic of China*
[14]*Helmholtz Institute Mainz, Staudinger Weg 18, D-55099 Mainz, Germany*
[15]*Henan Normal University, Xinxiang 453007, People's Republic of China*
[16]*Henan University of Science and Technology, Luoyang 471003, People's Republic of China*
[17]*Henan University of Technology, Zhengzhou 450001, Peoples Republic of China*
[18]*Huangshan College, Huangshan 245000, People's Republic of China*
[19]*Hunan Normal University, Changsha 410081, People's Republic of China*
[20]*Hunan University, Changsha 410082, People's Republic of China*
[21]*Indian Institute of Technology Madras, Chennai 600036, India*
[22]*Indiana University, Bloomington, Indiana 47405, USA*
[23a]*INFN Laboratori Nazionali di Frascati, I-00044 Frascati, Italy*
[23b]*INFN Sezione di Perugia, I-06100 Perugia, Italy*
[23c]*University of Perugia, I-06100 Perugia, Italy*
[24a]*INFN Sezione di Ferrara, I-44122 Ferrara, Italy*
[24b]*University of Ferrara, I-44122 Ferrara, Italy*
[25]*Institute of Modern Physics, Lanzhou 730000, People's Republic of China*
[26]*Institute of Physics and Technology, Peace Avenue 54B, Ulaanbaatar 13330, Mongolia*
[27]*Jilin University, Changchun 130012, People's Republic of China*
[28]*Johannes Gutenberg University of Mainz, Johann-Joachim-Becher-Weg 45, D-55099 Mainz, Germany*
[29]*Joint Institute for Nuclear Research, 141980 Dubna, Moscow region, Russia*
[30]*Justus-Liebig-Universitaet Giessen, II. Physikalisches Institut, Heinrich-Buff-Ring 16, D-35392 Giessen, Germany*
[31]*Lanzhou University, Lanzhou 730000, People's Republic of China*
[32]*Liaoning Normal University, Dalian 116029, People's Republic of China*
[33]*Liaoning University, Shenyang 110036, People's Republic of China*
[34]*Nanjing Normal University, Nanjing 210023, People's Republic of China*
[35]*Nanjing University, Nanjing 210093, People's Republic of China*
[36]*Nankai University, Tianjin 300071, People's Republic of China*
[37]*National Centre for Nuclear Research, Warsaw 02-093, Poland*
[38]*North China Electric Power University, Beijing 102206, People's Republic of China*
[39]*Peking University, Beijing 100871, People's Republic of China*
[40]*Qufu Normal University, Qufu 273165, People's Republic of China*
[41]*Shandong Normal University, Jinan 250014, People's Republic of China*

[42]*Shandong University, Jinan 250100, People's Republic of China*
[43]*Shanghai Jiao Tong University, Shanghai 200240, People's Republic of China*
[44]*Shanxi Normal University, Linfen 041004, People's Republic of China*
[45]*Shanxi University, Taiyuan 030006, People's Republic of China*
[46]*Sichuan University, Chengdu 610064, People's Republic of China*
[47]*Soochow University, Suzhou 215006, People's Republic of China*
[48]*South China Normal University, Guangzhou 510006, People's Republic of China*
[49]*Southeast University, Nanjing 211100, People's Republic of China*
[50]*State Key Laboratory of Particle Detection and Electronics, Beijing 100049, Hefei 230026, People's Republic of China*
[51]*Sun Yat-Sen University, Guangzhou 510275, People's Republic of China*
[52]*Suranaree University of Technology, University Avenue 111, Nakhon Ratchasima 30000, Thailand*
[53]*Tsinghua University, Beijing 100084, People's Republic of China*
[54a]*Turkish Accelerator Center Particle Factory Group, Istanbul Bilgi University, HEP Res. Cent., 34060 Eyup, Istanbul, Turkey*
[54b]*Turkish Accelerator Center Particle Factory Group, Near East University, Nicosia, North Cyprus, Mersin 10, Turkey*
[55]*University of Chinese Academy of Sciences, Beijing 100049, People's Republic of China*
[56]*University of Groningen, NL-9747 AA Groningen, Netherlands*
[57]*University of Hawaii, Honolulu, Hawaii 96822, USA*
[58]*University of Jinan, Jinan 250022, People's Republic of China*
[59]*University of Manchester, Oxford Road, Manchester M13 9PL, United Kingdom*
[60]*University of Minnesota, Minneapolis, Minnesota 55455, USA*
[61]*University of Muenster, Wilhelm-Klemm-Street 9, 48149 Muenster, Germany*
[62]*University of Oxford, Keble Rd, Oxford OX13RH, United Kingdom*
[63]*University of Science and Technology Liaoning, Anshan 114051, People's Republic of China*
[64]*University of Science and Technology of China, Hefei 230026, People's Republic of China*
[65]*University of South China, Hengyang 421001, People's Republic of China*
[66]*University of the Punjab, Lahore-54590, Pakistan*
[67a]*University of Turin, I-10125 Turin, Italy*
[67b]*University of Eastern Piedmont, I-15121 Alessandria, Italy*
[67c]*INFN, I-10125 Turin, Italy*
[68]*Uppsala University, Box 516, SE-75120 Uppsala, Sweden*
[69]*Wuhan University, Wuhan 430072, People's Republic of China*
[70]*Xinyang Normal University, Xinyang 464000, People's Republic of China*
[71]*Zhejiang University, Hangzhou 310027, People's Republic of China*
[72]*Zhengzhou University, Zhengzhou 450001, People's Republic of China*

(Received 5 November 2021; accepted 2 February 2022; published 24 February 2022)

[a]Also at the Moscow Institute of Physics and Technology, Moscow 141700, Russia.
[b]Also at the Novosibirsk State University, Novosibirsk, 630090, Russia.
[c]Also at the NRC "Kurchatov Institute", PNPI, 188300 Gatchina, Russia.
[d]Also at Goethe University Frankfurt, 60323 Frankfurt am Main, Germany.
[e]Also at Key Laboratory for Particle Physics, Astrophysics and Cosmology, Ministry of Education; Shanghai Key Laboratory for Particle Physics and Cosmology; Institute of Nuclear and Particle Physics, Shanghai 200240, People's Republic of China.
[f]Also at Key Laboratory of Nuclear Physics and Ion-beam Application (MOE) and Institute of Modern Physics, Fudan University, Shanghai 200443, People's Republic of China.
[g]Also at Harvard University, Department of Physics, Cambridge, Massachusetts 02138, USA.
[h]Also at State Key Laboratory of Nuclear Physics and Technology, Peking University, Beijing 100871, People's Republic of China.
[i]Also at School of Physics and Electronics, Hunan University, Changsha 410082, China.
[j]Also at Guangdong Provincial Key Laboratory of Nuclear Science, Institute of Quantum Matter, South China Normal University, Guangzhou 510006, China.
[k]Also at Frontiers Science Center for Rare Isotopes, Lanzhou University, Lanzhou 730000, People's Republic of China.
[l]Also at Lanzhou Center for Theoretical Physics, Lanzhou University, Lanzhou 730000, People's Republic of China.
[m]Currently at Istinye University, 34010 Istanbul, Turkey.

Using 6.32 fb^{-1} of e^+e^- collision data recorded by the BESIII detector at center-of-mass energies between 4.178 to 4.226 GeV, we present the first measurement of the decay $D_s^+ \to f_0(980)e^+\nu_e$, $f_0(980) \to \pi^0\pi^0$. The product branching fraction of $D_s^+ \to f_0(980)e^+\nu_e, f_0(980) \to \pi^0\pi^0$ is measured to be $(7.9 \pm 1.4_{\rm stat} \pm 0.4_{\rm syst}) \times 10^{-4}$, with a statistical significance of 7.8σ. Furthermore, the upper limits on the product branching fractions of $D_s^+ \to f_0(500)e^+\nu_e$ with $f_0(500) \to \pi^0\pi^0$ and the branching fraction of $D_s^+ \to K_S^0K_S^0e^+\nu_e$ are set to be 7.3×10^{-4} and 3.8×10^{-4} at 90% confidence level, respectively. Our results provide valuable inputs to the understanding of the structures of light scalar mesons.

DOI: 10.1103/PhysRevD.105.L031101

The constituent quark model has been strikingly successful, but the nontrivial quark structures of scalar mesons below 1 GeV, $f_0(500)$, $f_0(980)$, and $a_0(980)^{0(\pm)}$ (briefly denoted with σ, f_0, and $a_0^{0(\pm)}$, respectively), are not completely classified [1]. Many theoretical hypotheses, such as the tetraquark states [2–13], and two-meson bound states [14–18], have been proposed for these light scalar mesons but with controversial results. Identifying the correct hypothesis is key to exploring chiral-symmetry-breaking mechanisms of nonperturbative QCD in low-energy region [3]. Therefore, conclusive experimental results are required to interpret these states.

Semileptonic charm meson decays provide a clean environment to study scalar mesons [19–25]. Experimentally, the BESIII collaboration has reported the measurements of $D^{0(+)} \to a_0^{-(0)}e^+\nu_e$, and $D^+ \to f_0/\sigma e^+\nu_e$ with $f_0/\sigma \to \pi^+\pi^-$ [26,27], and the search of $D_s^+ \to a_0^0e^+\nu_e$ [28]. The CLEO collaboration has also reported the measurement of $D_s^+ \to f_0e^+\nu_e$ with $f_0 \to \pi^+\pi^-$ [29]. On the other hand, theoretical studies of neutral channels ($f_0 \to \pi^0\pi^0$) are rare compared to those of charged channels. Like charged channels, the branching fractions (BFs) of the semileptonic D_s^+ decays into light scalar mesons in their decay to neutral channels and the $\pi^0\pi^0$ invariant mass spectrum aid in understanding the nontrivial nature of light scalar mesons [4,11,20,25]. However, unlike charged channels, there is no background from $\rho(770)^0 \to \pi^+\pi^-$, thereby providing an ideal environment to study f_0/σ. Therefore, it is of great interest to study this kind of decays in experiment.

In addition, the *BABAR* collaboration claimed that a possible $f_0 \to K^+K^-$ contribution is found under the dominant decay $D_s^+ \to \phi e^+\nu_e$ in the study of $D_s^+ \to K^+K^-e^+\nu_e$ [30]. On the contrary, no other collaboration reported significant $f_0 \to K^+K^-$ signal in the same decay [1]. We report the first search for the neutral channel $D_s^+ \to K_S^0K_S^0e^+\nu_e$, associated with $f_0 \to K_S^0K_S^0$, avoiding heavy contamination from $\phi \to K^+K^-$ decays. Throughout this paper, charge conjugate channels are always implied.

The BESIII detector [31,32] records symmetric e^+e^- collisions provided by the BEPCII storage ring [33]. The cylindrical core of the BESIII detector covers 93% of the full solid angle and consists of a helium-based multilayer drift chamber (MDC), a plastic scintillator time-of-flight system (TOF), and a CsI(Tl) electromagnetic calorimeter (EMC), which are all enclosed in a superconducting solenoidal magnet providing a 1.0 T magnetic field. The charged-particle momentum resolution at 1 GeV$/c$ is 0.5%, and the dE/dx resolution is 6% for electrons from Bhabha scattering. The EMC measures photon energies with a resolution of 2.5% (5%) at 1 GeV in the barrel (end cap) region. The time resolution in the TOF barrel region is 68 ps, while that in the end cap region is 110 ps. The end cap TOF system was upgraded in 2015 using multi-gap resistive plate chamber technology, providing a time resolution of 60 ps [34].

The analysis is performed based on data samples corresponding to an integrated luminosity of 6.32 fb^{-1} at $\sqrt{s} =$ 4.178, 4.189, 4.199, 4.209, 4.219, and 4.226 GeV [35]. The signal events are selected from the process $e^+e^- \to D_s^{*\pm}D_s^{\mp} \to \gamma D_s^+D_s^-$. A GEANT4-based [36] Monte Carlo (MC) simulation sample is used to determine detection efficiencies and to estimate background processes. The simulation models the beam energy spread and initial state radiation (ISR) in the e^+e^- annihilations with the generator KKMC [37]. The inclusive MC sample includes the production of open charm processes, the ISR production of vector charmonium(like) states, and the continuum processes incorporated in KKMC [37]. The known decay modes are modeled with EvtGen [38] using BFs taken from the Particle Data Group [1], and the remaining unknown charmonium decays are modeled with LundCharm [39]. Final state radiation (FSR) from charged final state particles is incorporated using PHOTOS [40]. The signal detection efficiencies and signal shapes are obtained from signal MC samples. In the signal MC sample, the D_s^- decays generically and the signal D_s^+ decays to $\pi^0\pi^0e^+\nu_e$ or $K_S^0K_S^0e^+\nu_e$ according to the generators described below. The form factor $\mathcal{FF}$ is parametrized as [41,42]

$$\mathcal{FF} = p_{\rm had}m_{D_s}\frac{\mathcal{A}}{1-\frac{q^2}{m_A^2}}, \tag{1}$$

where q^2 is the invariant mass squared of $e^+\nu_e$ system, $p_{\rm had}$ is magnitude of the three-momentum of the $\pi^0\pi^0/K_S^0K_S^0$ system in the D_s^+ rest frame, the pole mass m_A is expected to be $m_{D_{s1}} \sim 2.5$ GeV$/c^2$ [1], and m_{D_s} is the nominal D_s^+ mass [1]. The amplitude $\mathcal{A}$ for the $f_0(980)$ resonance is parametrized by the Flatte formula with parameters fixed to the LHCb measurement [43], that for the σ resonance is described by the Bugg lineshape [44], and that in $D_s^+ \to K_S^0 K_S^0 e^+\nu_e$ signal MC sample is set to be one.

The signal process $e^+e^- \to D_s^{*+}D_s^- + \text{c.c.} \to \gamma D_s^+ D_s^- + \text{c.c.}$ allows studying semileptonic D_s^+ decays with a tag technique [45,46] since the neutrino is the only one particle undetected. There are two types of samples used in the tag technique: single tag (ST) and double tag (DT). In the ST sample, a D_s^- meson is reconstructed through a particular hadronic decay without any requirement on the remaining measured charged tracks and EMC showers. In the DT sample, a D_s^-, designated as "tag," is reconstructed through a hadronic decay mode first, and then a D_s^+, designated as the "signal," and the transition photon from the $D_s^{*\pm} \to \gamma D_s^\pm$ decay are reconstructed with the remaining tracks and EMC showers. The BF of the signal decay is given by [28]

$$\mathcal{B}_{\rm sig} = \frac{N_{\rm total}^{\rm DT}}{\mathcal{B}_\gamma \sum_{\alpha,i} N_{\alpha,i}^{\rm ST} \epsilon_{\alpha,i}^{\rm DT}/\epsilon_{\alpha,i}^{\rm ST}}, \qquad (2)$$

where α represents various tag modes, i denotes different $\sqrt{s}$, $\epsilon_{\alpha,i}^{\rm DT(ST)}$ denotes the DT (ST) reconstruction efficiencies, $\mathcal{B}_\gamma$ represents the BF of $D_s^* \to \gamma D_s$, $N_{\rm total}^{\rm DT}$ is the signal yield for all six data sets, and $N_{\alpha,i}^{\rm ST}$ is the ST yields for various tag modes. The tag candidates are reconstructed with charged K and π, π^0, $\eta^{(\prime)}$, and K_S^0 mesons in nine tag modes, $D_s^- \to K_S^0 K^-$, $K^+K^-\pi^-$, $K_S^0 K^-\pi^0$, $K^+K^-\pi^-\pi^0$, $K_S^0 K^-\pi^-\pi^+$, $K_S^0 K^+\pi^-\pi^-$, $\pi^-\pi^-\pi^+$, $\pi^-\eta'$, and $K^-\pi^+\pi^-$. Requirements on the recoiling mass are applied to the tag candidates in order to identify the process $e^+e^- \to D_s^{*\pm}D_s^\mp$. If there are multiple candidates for a tag mode, the one with recoiling mass closest to the nominal $D_s^{*\pm}$ mass [1] is chosen. A detailed description of the requirements on the mass and the recoiling mass of tagged D_s^-, and the selection criteria for charged and neutral particle candidates is provided in Ref. [28]. The ST yields of data for tag modes $N_{\alpha,i}^{\rm ST}$ are determined from fitting to the tag D_s^- invariant mass ($M_{\rm tag}$) distributions [47]. The signal shape is modeled with the MC-simulated shape convolved with a Gaussian function, and the background is parameterized as a second-order Chebyshev function. The efficiencies ϵ for ST are obtained from the inclusive MC samples [47].

After a tag D_s^- is identified, the signal decays are selected recoiling against the tag side, requiring that there is no track other than those accounted for in the tagged D_s^-, the positron, and the semileptonic-side hadrons ($N_{\rm char}^{\rm extra} = 0$). A joint kinematic fit, in which four-momentum of the missing neutrino needs to be determined, is performed to select the best transition photon candidate from $D_s^{*\pm} \to \gamma D_s^\pm$. The fit includes: The total four-momentum of reconstructed particles and the missing neutrino is constrained to the four-momentum of e^+e^- system; invariant masses of the two π^0/K_S^0 candidates, the D_s^- tag, the D_s^+ signal, and the $\gamma D_s^\pm$ are constrained to the corresponding nominal masses [1]. The transition photon candidate leading to the minimum χ^2 of the joint kinematic fit is chosen. Furthermore, the largest energy of the remaining EMC showers that are not used to in the event reconstruction, $E_{\gamma,\max}^{\rm extra}$, is required to be less than 0.2 GeV to suppress backgrounds with photon(s). The square of the recoil mass against the transition photon and the D_s^- tag ($M_{\rm rec}^2$) is expected to peak at the nominal $D_s^\pm$ meson mass-squared before the kinematic fit for signal $D_s^{*\pm}D_s^\mp$ events. Therefore, $M_{\rm rec}^2$ is required to satisfy $3.75\ {\rm GeV}^2/c^4 < M_{\rm rec}^2 < 4.05\ {\rm GeV}^2/c^4$ to suppress the backgrounds from non-$D_sD_s^*$ processes. The missing neutrino is inferred by the missing mass squared (MM^2), defined as

$$MM^2 = \frac{1}{c^2}(p_{\rm cm} - p_{\rm tag} - p_{\rm had} - p_e - p_\gamma)^2, \qquad (3)$$

where $p_{\rm cm}$ is the four-momentum of the e^+e^- center-of-mass system, $p_{\rm tag}$ for the tag D_s^-, $p_{{\rm had}(e)}$ for the semileptonic-side hadrons (positron), and p_γ for the transition photon from the $D_s^{*\pm}$ decay. To partially recover the energy lost due to FSR and bremsstrahlung, the four-momenta of photon(s) within 5° of the initial positron direction are added to the positron four-momentum measured by the MDC. The invariant mass distributions of semileptonic-side hadrons of the selected candidates for $D_s^+ \to \pi^0\pi^0 e^+\nu_e$ and $D_s^+ \to K_S^0 K_S^0 e^+\nu_e$ are shown in Fig. 1. Notable f_0 signals are found in the $\pi^0\pi^0$ mass distribution while no significant signals of $\sigma \to \pi^0\pi^0$ and $f_0 \to K_S^0 K_S^0$ are observed. The background is mostly caused by miscellaneous backgrounds with multiple photons.

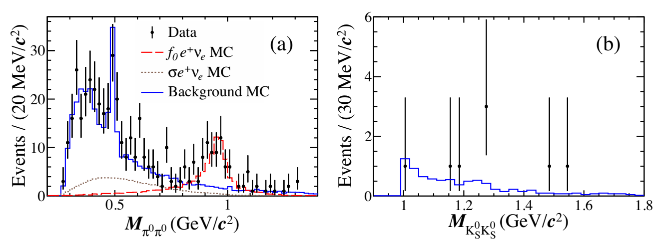

FIG. 1. Invariant mass distributions of semileptonic-side hadrons of the selected candidates for (a) $D_s^+ \to \pi^0\pi^0 e^+\nu_e$ and (b) $D_s^+ \to K_S^0 K_S^0 e^+\nu_e$. The points with error bars are data. The blue solid lines are the MC-simulated backgrounds. The peak around 0.5 GeV$/c^2$ in (a) is caused by the decay $D_s^+ \to K_S^0(\to \pi^0\pi^0)e^+\nu_e$. The red dashed and brown dotted lines are signal MC samples of $D_s^+ \to f_0(980)e^+\nu_e$ and $D_s^+ \to \sigma e^+\nu_e$, respectively, which are normalized arbitrarily for visualization purposes. A cut on missing mass squared, $|MM^2| < 0.15\ {\rm GeV}^2/c^4$, is applied.

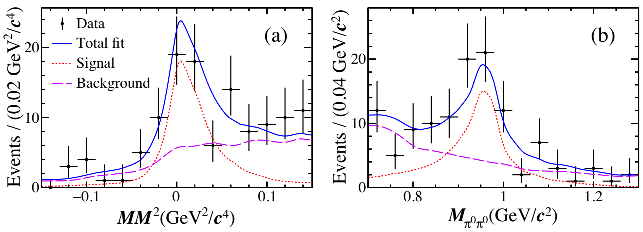

FIG. 2. Projection on (a) MM^2 and (b) $M_{\pi^0\pi^0}$ of the two-dimensional fit to the selected candidates for $D_s^+ \to \pi^0\pi^0 e^+\nu_e$. The data are represented by points with error bars, the total fit result by blue solid lines, signal by red dashed lines, and background by violet long-dashed lines.

A two-dimensional unbinned maximum likelihood fit to the MM^2 versus $M_{\pi^0\pi^0}$ distribution is performed to extract the DT yield of $D_s^+ \to f_0 e^+\nu_e, f_0 \to \pi^0\pi^0$. The signal and background components are described by the simulated shape from the signal and inclusive MC samples, respectively, using a kernel estimation method [48] implemented in RooFit [49]. The fit result is shown in Fig. 2. The obtained signal yields is $N_{\rm total}^{\rm DT} = 54.8 \pm 10.1$ with a statistical significance of 7.8σ. Using the DT efficiencies from the signal MC samples (see Ref. [47]), and $\mathcal{B}_\gamma$, the resulting $\mathcal{B}(D_s^+ \to f_0 e^+\nu_e, f_0 \to \pi^0\pi^0)$ is $(7.9 \pm 1.4_{\rm stat} \pm 0.4_{\rm syst}) \times 10^{-4}$. The second uncertainty is systematic, which are described in the following.

Since no significant signals are observed for the decays $D_s^+ \to \sigma e^+\nu_e$ with $\sigma \to \pi^0\pi^0$ and $D_s^+ \to K_S^0 K_S^0 e^+\nu_e$, the upper limits of the BFs for these decays are determined. The candidate events for the former decay are required to satisfy $M_{\pi^0\pi^0} < 0.66~{\rm GeV}/c^2$. A veto $0.458 < M_{\pi^0\pi^0} < 0.520~{\rm GeV}/c^2$ is applied to suppress the background from $D_s^+ \to K_S^0(\to \pi^0\pi^0)e^+\nu_e$. Unbinned maximum-likelihood fits are performed to the corresponding MM^2 distributions The signal and background are modeled by the simulated shapes obtained from the signal and inclusive MC samples, respectively. The MM^2 distributions and the likelihoods of fit results as functions of assumed BFs are presented in Fig. 3. The upper limits, set at 90% C.L., of the BFs of $D_s^+ \to \sigma e^+\nu_e, \sigma \to \pi^0\pi^0$ and $D_s^+ \to K_S^0 K_S^0 e^+\nu_e$ are 7.3×10^{-4} and 3.8×10^{-4}, respectively. The method to incorporate systematic uncertainty is discussed in the following.

The sources of the systematic uncertainties for the BF measurement of $D_s^+ \to f_0 e^+\nu_e$, as summarized in Table I, are described below. Note that most systematic uncertainties on the tag side cancel due to the DT technique. Any residual effects are negligible.

The uncertainty in the total number of the ST D_s^- mesons is assigned to be 0.4% by examining the changes of the fit yields when varying the signal shape, background shape, and taking into account the background fluctuation in the fit. The uncertainty from the quoted BF of $D_s^* \to \gamma D_s$ is 0.7% [1]. The systematic uncertainties from tracking and PID efficiencies of e^+ are assigned as 1.0% for each by using radiative Bhabha events. The systematic uncertainties from reconstruction efficiencies of γ and π^0 are studied by using control samples of the decay $J/\psi \to \pi^+\pi^-\pi^0$ [50,51] and the process $e^+e^- \to K^+K^-\pi^+\pi^-\pi^0$, respectively. A conservative 2%(1%) systematic uncertainty is assigned for each π^0 (the transition photon) in the analysis of $D_s^+ \to \sigma e^+\nu_e$, since no significant signal is available to check the data-MC consistency. As for the analysis of

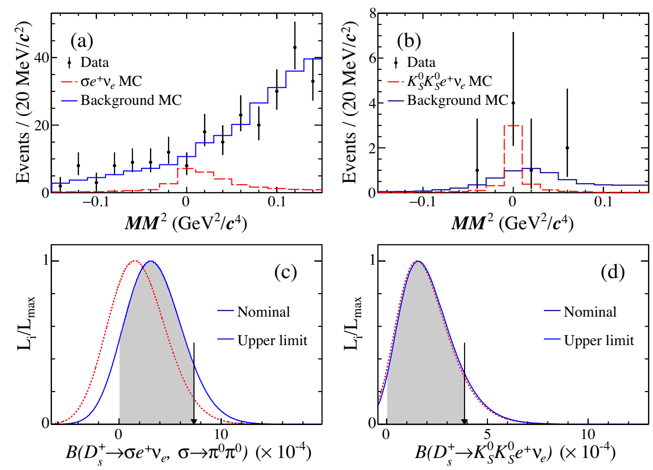

FIG. 3. (top) MM^2 distributions and (bottom) likelihood distributions versus BF for (left) $D_s^+ \to \sigma e^+\nu_e, \sigma \to \pi^0\pi^0$ and (right) $D_s^+ \to K_S^0 K_S^0 e^+\nu_e$. The points with error bars are data, the blue solid lines are the MC-simulated backgrounds, and the red dashed lines show the MC-simulated signal shapes in (a, b). The signal shapes are normalized using an appropriate scaling factor chosen to visualize the shape and position of the signal. The red dashed lines in (c, d) are the likelihood curves for the nominal fit models, while the blue solid lines represent the likelihood curves that gives the upper limits after incorporating the systematic uncertainties. The black arrows indicate the results corresponding to 90% C.L.

TABLE I. The systematic uncertainties (%) in the BF measurements. Uncertainties associated with background shapes for $\sigma e^+\nu_e$ and $K_S^0 K_S^0 e^+\nu_e$ are additive in the upper limit measurements and not listed in this table.

Source	$f_0 e^+\nu_e$	$\sigma e^+\nu_e$	$K_S^0 K_S^0 e^+\nu_e$
D_s^- yield	0.4	0.4	0.4
$\mathcal{B}(D^{*\pm} \to \gamma D^{*\pm})$	0.7	0.7	0.7
e^+ tracking efficiency	1.0	1.0	1.0
e^+ PID efficiency	1.0	1.0	1.0
γ and π^0 reconstruction	2.6	5.0	1.0
K_S^0 reconstruction	...	...	3.0
$E_{\gamma,\rm max}^{\rm extra} < 0.2$ GeV	0.7	0.7	0.5
$N_{\rm char}^{\rm extra} = 0$	0.8	0.8	0.9
MC statistics	0.5	0.5	0.5
Signal model	1.3	3.3	8.8
Background shape	3.0	See text	See text
Total	4.7	6.3	9.5

$D_s^+ \to f_0 e^+\nu_e$, a momentum-weighted correction factor for each π^0 is calculated to be 99.4% and the residual uncertainty of 0.8% is assigned as the corresponding systematic uncertainty along with a 1% systematic uncertainty for the transition photon. The uncertainties of the $E_{\gamma,\max}^{\rm extra} < 0.2$ GeV and $N_{\rm char}^{\rm extra} = 0$ requirements are assigned as 0.7% and 0.8%, respectively, by analyzing DT hadronic events of $\pi^\pm\pi^0\eta$. The uncertainty due to the limited MC statistics is obtained by $\sqrt{\sum_\alpha (f_\alpha \frac{\delta_{\epsilon_\alpha}}{\epsilon_\alpha})^2}$, where f_α is the tag yield fraction in data, and ϵ_α and δ_{ϵ_α} are the signal efficiency and the corresponding uncertainty of tag mode α, respectively. The systematic uncertainty associated with signal models is studied by replacing the parameters of f_0 from LHCb [43] by those from BES [52] in generating the signal MC sample. The difference of the measured BFs, where the effects of the signal efficiencies and the two-dimensional signal shape have been taken into account, is assigned as the associated systematic uncertainty. The background shape is altered by varying the relative fractions of major backgrounds from $e^+e^- \to q\bar{q}$ and non-$D_s^{*+}D_s^-$ open-charm processes within 30% according to the uncertainties of their input crossing section in the inclusive MC sample. The effects caused by the smoothing parameter of the kernel estimation method [48,49] is negligible. The largest change is taken as the corresponding systematic uncertainty.

The sources of systematic uncertainties on the upper limit measurements are classified into two types: additive (σ_n) and multiplicative (σ_ϵ).

Additive uncertainty is dominated by the background shape description. The systematic uncertainty is studied by altering the nominal MC background shape with two methods. First, alternative simulated shapes are used, where the relative fractions of the dominant backgrounds from $e^+e^- \to q\bar{q}$ and non-$D_s^{*\pm}D_s^\mp$ open-charm processes are varied within 30% according to the uncertainties of their input crossing section in the inclusive MC sample. Second, the alternative background shapes are obtained from the inclusive MC sample using the kernel estimation method [48,49] with the smoothing parameter varied to be 0, 1, and 2.

Multiplicative uncertainties, as summarized in Table I, are related to the efficiency determination and the quoted BFs. All systematic uncertainties are the same as those for $D_s^+ \to f_0 e^+\nu_e$ except for the following. The uncertainty for the K_S^0 reconstruction efficiency is assigned as 1.5% per K_S^0 using control samples of $J/\psi \to K_S^0 K^\pm \pi^\mp$ and $\phi K_S^0 K^\pm \pi^\mp$ decays. The uncertainties of the $E_{\gamma,\max}^{\rm extra} < 0.2$ GeV and $N_{\rm char}^{\rm extra} = 0$ requirements in the $D_s^+ \to K_S^0 K_S^0 e^+\nu_e$ study are assigned as 0.5% and 0.9%, respectively, by analyzing DT hadronic events of $D_s^+ \to K^+K^-\pi^\pm$ and $K_S^0 K^\pm$. The systematic uncertainty of the σ modeling is considered by replacing the lineshape of σ in the signal MC sample with a conventional relativistic Breit-Wigner function with the mass and width fixed to the BES measurements [53]. The systematic uncertainty related to the $K_S^0 K_S^0 e^+\nu_e$ model is estimated by replacing the nominal model in the signal MC sample by a uniform distribution in phase space.

The additive uncertainty is taken into account by extracting likelihood distributions using different alternative background shapes and the one resulting the most conservative upper limit is chosen. Then, the multiplicative systematic uncertainty is incorporated in the calculation of the upper limit via [54,55]

$$L(\mathcal{B}) \propto \int_0^1 L\left(\mathcal{B}\frac{\epsilon}{\epsilon_0}\right) \exp\left[\frac{-(\epsilon/\epsilon_0 - 1)^2}{2(\sigma_\epsilon)^2}\right] d\epsilon, \qquad (4)$$

where $L(\mathcal{B})$ is the likelihood distribution as a function of BF; ϵ is the expected efficiency and ϵ_0 is the averaged MC-estimated efficiency.

In summary, the first BF measurement of $D_s^+ \to f_0 e^+\nu_e, f_0 \to \pi^0\pi^0$ and searches for $D_s^+ \to \sigma e^+\nu_e, \sigma \to \pi^0\pi^0$ and $D_s^+ \to K_S^0 K_S^0 e^+\nu_e$ are performed using 6.32 fb^{-1} of data taken at $\sqrt{s} = 4.178$–4.226 GeV with the BESIII detector.

The BF of $D_s^+ \to f_0 e^+\nu_e, f_0 \to \pi^0\pi^0$ is determined to be $(7.9 \pm 1.4_{\rm stat} \pm 0.4_{\rm syst}) \times 10^{-4}$. According to isospin symmetry expectation $\frac{\mathcal{B}(f_0\to\pi^0\pi^0)}{\mathcal{B}(f_0\to\pi^+\pi^-)} = 0.5$, our result is consistent with the measurement of $D_s^+ \to f_0 e^+\nu_e$ with $f_0 \to \pi^+\pi^-$ by the CLEO collaboration [29]. An upper limit on the BF of $D_s^+ \to \sigma e^+\nu_e, \sigma \to \pi^0\pi^0$ is set to be 7.3×10^{-4} at 90% C.L. This upper limit is an overestimation due to omitting the non-σ contribution in the region of $M_{\pi^0\pi^0} < 0.66$ GeV$/c^2$. Our results agree with the statement that the $s\bar{s} \to \sigma$ transition is negligibly small in comparison with that of $s\bar{s} \to f_0$ given by Refs. [20,23], which follow the four-quark structure or mesonmeson interaction hypothesis for f_0 and σ mesons. Furthermore, the upper limit on $\mathcal{B}(D_s^+ \to K_S^0 K_S^0 e^+\nu_e)$ is set to be 3.8×10^{-4} at 90% C.L., indicating that contribution from $\mathcal{B}(f_0 \to K\bar{K})$ is not comparable to $\mathcal{B}(f_0 \to \pi\pi)$ in semileptonic D_s^+ decays. Assuming $\mathcal{B}(f_0 \to \pi^0\pi^0)$ contributes one third of the f_0 decays, our results leads to $\mathcal{B}(D_s^+ \to f_0 e^+\nu_e) = (2.4 \pm 0.4) \times 10^{-3}$, which is consistent with the prediction given by Refs. [23,24] when assuming f_0 to be the admixture of $s\bar{s}$ and other light quark-antiquark pairs.

The BESIII collaboration thanks the staff of BEPCII and the IHEP computing center for their strong support. This work is supported in part by National Key R&D Program of China under Contracts No. 2020YFA0406400, No. 2020YFA0406300; National Natural Science Foundation of China (NSFC) under Contracts No. 11625523, No. 11635010, No. 11735014, No. 11822506, No. 11835012, No. 11875054, No. 11935015, No. 11935016, No. 11935018, No. 11961141012, No. 12022510, No. 12025502, No. 12035009, No. 12035013, No. 12061131003, No. 12192260, No. 12192261, No. 12192262, No. 12192263, No. 12192264, No. 12192265; the Chinese Academy of Sciences (CAS) Large-Scale Scientific Facility Program; Joint Large-Scale Scientific Facility Funds of the NSFC and CAS under Contracts No. U2032104, No. U1732263, No. U1832207; CAS Key Research Program of Frontier Sciences under Contract No. QYZDJ-SSW-SLH040; 100 Talents Program of CAS; The Institute of Nuclear and Particle Physics (INPAC), and Shanghai Key Laboratory for Particle Physics and Cosmology; ERC under Contract No. 758462; European Union Horizon 2020 research and innovation programme under Contract No. Marie Sklodowska-Curie grant agreement No. 894790; German Research Foundation DFG under Contracts No. 443159800, Collaborative Research Center No. CRC 1044, No. FOR 2359, No. FOR 2359, No. GRK 214; Istituto Nazionale di Fisica Nucleare, Italy; Ministry of Development of Turkey under Contract No. DPT2006K-120470; National Science and Technology fund; Olle Engkvist Foundation under Contract No. 200-0605; STFC (United Kingdom); The Knut and Alice Wallenberg Foundation (Sweden) under Contract No. 2016.0157; The Royal Society, UK under Contracts No. DH140054, No. DH160214; The Swedish Research Council; U.S. Department of Energy under Contracts No. DE-FG02-05ER41374, No. DE-SC-0012069.

[1] P. A. Zyla *et al.* (Particle Data Group), Prog. Theor. Exp. Phys. (**2020**), 083C01.
[2] X. D. Cheng, H. B. Li, B. Wei, Y. G. Xu, and M. Z. Yang, Phys. Rev. D **96**, 033002 (2017).
[3] R. L. Jaffe, Phys. Rev. D **15**, 267 (1977).
[4] N. N. Achasov, Nucl. Phys. **A728**, 425 (2003).
[5] J. R. Peláez, Phys. Rev. Lett. **92**, 102001 (2004).
[6] G.'t Hooft, G. Isidori, L. Maiani, A. D. Polosa, and V. Riquer, Phys. Lett. B **662**, 424 (2008).
[7] A. H. Fariborz, R. Jora, and J. Schechter, Phys. Rev. D **79**, 074014 (2009).
[8] S. Weinberg, Phys. Rev. Lett. **110**, 261601 (2013).
[9] N. N. Achasov and A. V. Kiselev, Phys. Rev. D **97**, 036015 (2018).
[10] H. C. Kim, K. S. Kim, M. K Cheoun, D. Jido, and M. Oka, Phys. Rev. D **99**, 014005 (2019).
[11] N. N. Achasov, J. V. Bennett, A. V. Kiselev, E. A. Kozyrev, and G. N. Shestakov, Phys. Rev. D **103**, 014010 (2021).
[12] Y. K. Hsiao, Y. Yu, and B. C. Ke, Eur. Phys. J. C **80**, 895 (2020).
[13] Y. Yu, Y. K. Hsiao, and B. C. Ke, Eur. Phys. J. C **81**, 1093 (2021).
[14] J. Weinstein and N. Isgur, Phys. Rev. Lett. **48**, 659 (1982).
[15] T. Branz, T. Gutschea, and V. Lyubovitskij, Eur. Phys. J. A **37**, 303 (2008).
[16] L. Y. Dai, X. G. Wang, and H. Q. Zheng, Commun. Theor. Phys. **58**, 410 (2012).
[17] L. Y. Dai and M. R. Pennington, Phys. Lett. B **736**, 11 (2014).
[18] T. Sekihara and S. Kumano, Phys. Rev. D **92**, 034010 (2015).
[19] W. Wang and C. D. Lu, Phys. Rev. D **82**, 034016 (2010).
[20] N. N. Achasov and A. V. Kiselev, Phys. Rev. D **86**, 114010 (2012).
[21] N. N. Achasov and A. V. Kiselev, Int. J. Mod. Phys. Conf. Ser. **35**, 1460447 (2014).
[22] W. Wang, Phys. Lett. B **759**, 501 (2016).
[23] T. Sekihara and E. Oset, Phys. Rev. D **92**, 054038 (2015).
[24] N. R. Soni, A. N. Gadaria, J. J. Patel, and J. N. Pandya, Phys. Rev. D **102**, 016013 (2020).
[25] N. N. Achasov, A. V. Kiselev, and G. N. Shestakov, Phys. Rev. D **102**, 016022 (2020).
[26] M. Ablikim *et al.* (BESIII Collaboration), Phys. Rev. Lett. **121**, 081802 (2018).
[27] M. Ablikim *et al.* (BESIII Collaboration), Phys. Rev. Lett. **122**, 062001 (2019).
[28] M. Ablikim *et al.* (BESIII Collaboration), Phys. Rev. D **103**, 092004 (2021).
[29] K. M. Ecklund *et al.* (CLEO Collaboration), Phys. Rev. D **80**, 052009 (2009).
[30] B. Aubert *et al.* (*BABAR* Collaboration), Phys. Rev. D **78**, 051101(R) (2008).
[31] M. Ablikim *et al.* (BESIII Collaboration), Nucl. Instrum. Methods Phys. Res., Sect. A **614**, 345 (2010).
[32] M. Ablikim *et al.* (BESIII Collaboration), Chin. Phys. C **44**, 040001 (2020).
[33] C. H. Yu *et al.*, *Proceedings of IPAC2016, Busan, Korea*, 2016, https://inspirehep.net/files/96083dc6a03caf20597ac-55b4500673a.
[34] X. Li *et al.*, Radiat. Detect. Technol. Methods **1**, 13 (2017); Y. X. Guo *et al.*, Radiat. Detect. Technol. Methods **1**, 15 (2017).
[35] M. Ablikim *et al.* (BESIII Collaboration), J. High Energy Phys. 06 (2021) 181.
[36] S. Agostinelli *et al.* (GEANT4 Collaboration), Nucl. Instrum. Methods Phys. Res., Sect. A **506**, 250 (2003).
[37] S. Jadach, B. F. L. Ward, and Z. Was, Phys. Rev. D **63**, 113009 (2001); Comput. Phys. Commun. **130**, 260 (2000).
[38] D. J. Lange, Nucl. Instrum. Methods Phys. Res., Sect. A **462**, 152 (2001); R. G. Ping, Chin. Phys. C **32**, 599 (2008).
[39] J. C. Chen, G. S. Huang, X. R. Qi, D. H. Zhang, and Y. S. Zhu, Phys. Rev. D **62**, 034003 (2000); R. L. Yang, R. G. Ping, and H. Chen, Chin. Phys. Lett. **31**, 061301 (2014).
[40] E. Richter-Was, Phys. Lett. B **303**, 163 (1993).
[41] P. del Amo Sanchez *et al.* (*BABAR* Collaboration), Phys. Rev. D **83**, 072001 (2011).

[42] C. L. Y. Lee, M. Lu, and M. B. Wise, Phys. Rev. D **46**, 5040 (1992).

[43] R. Aaij *et al.* (LHCb Collaboration), Phys. Rev. D **86**, 052006 (2012).

[44] D. V. Bugg, J. Phys. G **34**, 151 (2007).

[45] H. B. Li and X. R. Lyu, Natl. Sci. Rev. **8**, nwab181 (2021).

[46] J. Adler *et al.* (MARK-III Collaboration), Phys. Rev. Lett. **62**, 1821 (1989).

[47] See Supplemental Material at http://link.aps.org/supplemental/10.1103/PhysRevD.105.L031101 for additional analysis information.

[48] K. S. Cranmer, Comput. Phys. Commun. **136**, 198 (2001).

[49] R. Brun and F. Rademakers, Nucl. Instrum. Methods Phys. Res., Sect. A **389**, 81 (1997).

[50] M. Ablikim *et al.* (BESIII Collaboration), Eur. Phys. J. C **76**, 369 (2016).

[51] M. Ablikim *et al.* (BESIII Collaboration), Chin. Phys. C **40**, 113001 (2016).

[52] M. Ablikim *et al.* (BES Collaboration), Phys. Lett. B **607**, 243 (2005).

[53] M. Ablikim *et al.* (BES Collaboration), Phys. Lett. B **598**, 149 (2004).

[54] K. Stenson, arXiv:physics/0605236.

[55] X. X. Liu, X. R. Lyu, and Y. S. Zhu, Chin. Phys. C **39**, 113001 (2015).